Supplementary information

The preparation of NiV_3O_8/Ni composite via an in situ corrosion method and its use as a new sort of anode material for Li-ion battery

Shibing Ni,* Jianjun Ma, Xiaohu Lv, Xuelin Yang* and Lulu Zhang

College of Materials and Chemical Engineering, Collaborative Innovation Center for Energy Equipment of Three Gorges Region, Three Gorges University, 8 Daxue Road, Yichang, Hubei 443002, China.

E-mail: shibingni07@gmail.com

Experiments

Sample preparation

Glucose ($C_6H_{12}O_6 \cdot H_2O$) and V_2O_5 were analytical grade and purchased from Shanghai Chemical Reagents. Ni foam (100 PPI pore size, 380 g m^{-2} surface density, 1.5 mm thick) was purchased from Changsha Lyrun New Material corporation. In a typical procedure, Ni foam was firstly put into diluted hydrochloric acid ($HCl:H_2O$=1:10) until the solution changes into pea green to eliminate the surface oxide layer. Then it was ultrasonically washed with distilled water to remove the rudimental Cl^-. For fabrication of NiV_3O_8/Ni, 2 mmol V_2O_5 and 1mmol glucose were firstly dissolved in 30ml distilled water. After stirring for 20 minutes, the homogeneous yellowy suspension was transferred into a 50ml Teflon-lined autoclave. The pretreated Ni foams were placed into the autoclave, distilled water was

subsequently added up to 80% of its capacity. The autoclave was at last sealed and placed in an oven, heated at 160°C for 24h. After the reaction, the autoclave was cooled to room temperature. Finally, NiV_3O_8/Ni was obtained via annealing the deposited Ni foams at 400 °C in air for 5h with a heating rate of 3°C min^{-1}.

Structure and morphology characterization

The structure and morphology of the resulting products were characterized by X-Ray powder diffraction (Rigaku Ultima IV, Cu Kα radiation, λ=1.5406 Å) and field-emission scanning electron microscopy (FE-SEM JSM 7500F, JEOL).

Electrochemical characterization

For fabricating of Li-ion battery, the NiV_3O_8/Ni discs were dried at 120 °C for 24 h in vacuum oven. Coin-type cells (2025) of Li/1 M $LiPF_6$ in ethylene carbonate, dimethyl carbonate and diethyl carbonate (EC/DMC/DEC, 1:1:1 v/v/v)/NiV_3O_8/Ni disc (diameter of 14 mm) were assembled in an argon-filled dry box (MIKROUNA, Super 1220/750, H_2O<1.0 ppm, O_2<1.0 ppm). A Celgard 2400 microporous polypropylene was used as the separator membrane. The cells were tested in the voltage range between 0.02 and 3 V with a multichannel battery test system (LAND CT2001A). The Cyclic voltammetry (CV) measurement of the electrodes was carried out on a CHI660C electrochemical workstation at a scan rate of 0.2 mV s^{-1} between 0 and 3 V.

As shown in Fig. S1, XRD pattern of the sample prepared via electrochemical corrosion of Ni foam shows obvious diffraction peaks of $Ni(OH)_2$ and Ni (marked by ＊). For the sample prepared via the reduction of V_2O_5 by glucose under hydrothermal condition, diffraction peaks of VO_2 can be clearly seen. For the as-prepared sample (in experimental section), the diffraction peaks of VO_2 and $Ni(OH)_2$

can be found in the XRD pattern, which suggests the deposition of VO_2 and the formation of $Ni(OH)_2$ on Ni foam.
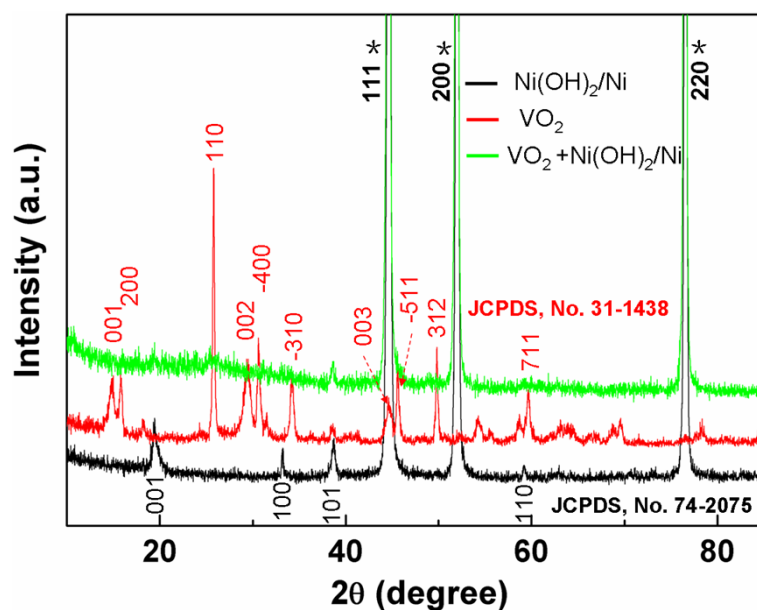

Fig. S1 XRD patterns of the samples prepared under different conditions. (Black curve: Ni foam after electrochemical corrosion; Red curve: the sample prepared via a hydrothermal method at 160 °C for 24h in the presence of 2 mmol V_2O_5 and 2mmol glucose; Green curve: the deposited Ni foam).

Fig. S2 is the XRD patterns of NiV_3O_8/Ni electrode after 1 and 100 cycles testing with charge state. As seen, no diffraction peaks other than Ni foams were detected for both curve a and curve b, which may be relevant to the transformation of NiV_3O_8 into amorphous phase during cycling. According to the XRD results, it can be deduced that the amorphous phase forms in the first cycle, maintaining amorphous state in the subsequent cycling.
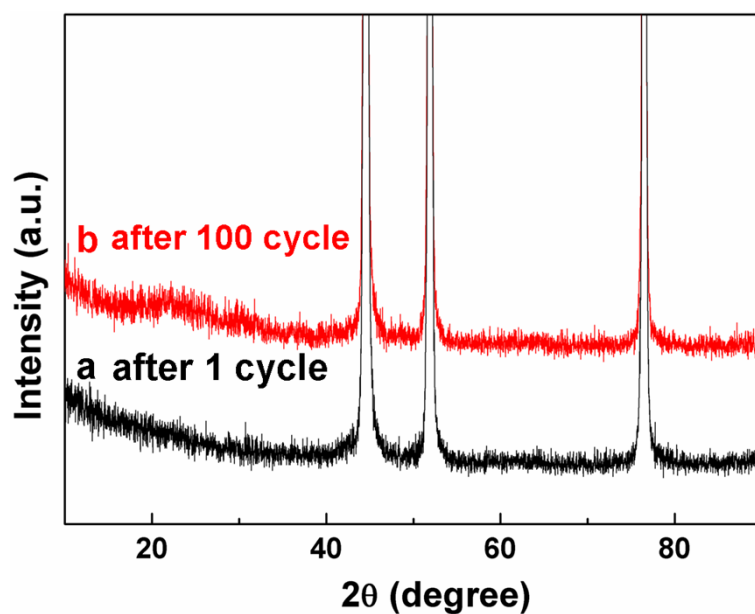
Fig. S2 XRD patterns of the NiV$_3$O$_8$/Ni electrode after 1 cycle (curve a) and 100 cycles (curve b) testing with charge state.

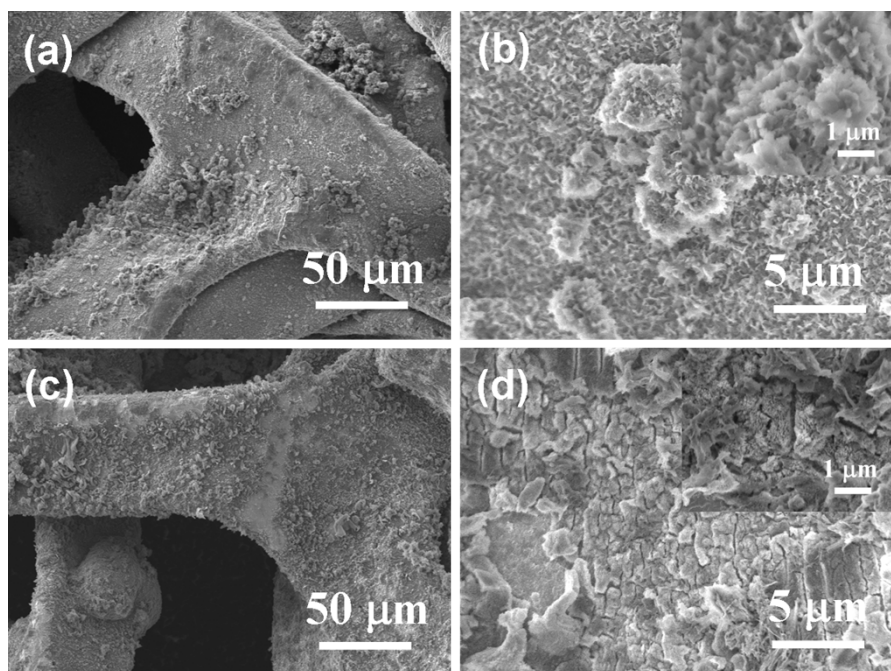Fig. S3 SEM images of NiV$_3$O$_8$/Ni electrode after different cycles with charge state. (a) low and (b) high magnification after 1 cycle. The insert of (b) is a magnified SEM image. (c) low and (d) high magnification after 100 cycles. The insert of (d) is a magnified SEM image.

SEM images of the NiV$_3$O$_8$/Ni electrode after different cycles with charge state is

shown in Fig. S3. As seen, 3D porous architecture of NiV_3O_8/Ni electrode is well preserved after cycling. After 1 cycle testing, the NiV_3O_8 shows porous architecture, which is composed of a large number of nanoparticles, being different from that of the as-prepared NiV_3O_8/Ni electrode with flake-like morphology. The morphology variation suggests a phase transition during the first cycle, which is in accordance with the XRD result in Fig. S2. The NiV_3O_8/Ni after 100 cycles exhibits block-like morphology, which differs much from that of the as-prepared electrode. However, these NiV_3O_8 blocks are porous, consisting of a large number of nano-sized particles.
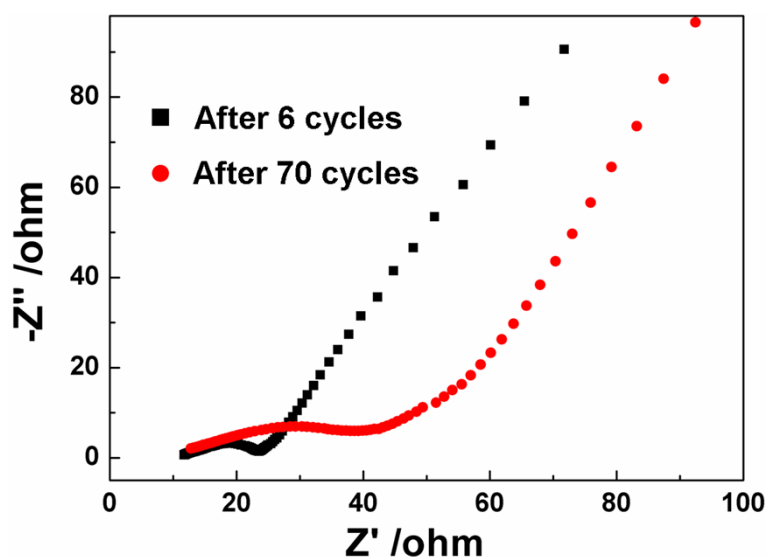

Fig. S4 AC impedance spectra of the NiV_3O_8/Ni electrode after different cycles with charge state.

Fig. S4 shows the electrochemical impedance spectra (EIS) of the NiV_3O_8/Ni electrode under different states. The semicircle in high-frequency can be attributed to the SEI film and/or contact resistance (Re), the medium-frequency semicircle is due to the charge-transfer impedance (Rct) on electrode/electrolyte interface, and the inclined line in low-frequency corresponds to the Li-ion diffusion process within electrodes [1]. As seen, similar value of Re under different state suggests good electrical contact between Ni foam and NiV_3O_8 in cycling. Rct for the NiV_3O_8/Ni

electrode after 70 cycles shows bigger value than that after 6 cycles, which is relevant to the structure destruction of the electrode in cycling. However, the slope of the inclined lines of NiV_3O_8/Ni electrode under different state shows similar value, which is relevant to the formation of nanosized NiV_3O_8 in cycling. In such situation, the integrated structure of the electrode changes along with cycling, but the primary particles show similar size and morphology in cycling.

[1] Y.J. Zhu, C.S. Wang, Novel CV for Phase Transformation Electrodes, The Journal of Physical Chemistry C, 115 (2011) 823-832.